Transcriptomal analysis of varicella-zoster virus infection using long oligonucleotide-based microarrays

Journal of General Virology (2005), **86**, 2673–2684 DOI 10.1099/vir.0.80946-0

Transcriptomal analysis of varicella-zoster virus infection using long oligonucleotide-based microarrays

Peter G. E. Kennedy,[1] Esther Grinfeld,[1] Marie Craigon,[2] Klemens Vierlinger,[2] Douglas Roy,[2] Thorsten Forster[2] and Peter Ghazal[2]

Correspondence
Peter G. E. Kennedy
P.G.Kennedy@clinmed.gla.ac.uk

[1]Glasgow University Department of Neurology, Southern General Hospital, Institute of Neurological Sciences, Glasgow G51 4TF, UK

[2]Scottish Centre for Genomic Technology and Informatics, Medical School, University of Edinburgh, Edinburgh EH16 4SB, UK

Varicella-zoster virus (VZV) is a human herpes virus that causes varicella as a primary infection and herpes zoster following reactivation of the virus from a latent state in trigeminal and spinal ganglia. In order to study the global pattern of VZV gene transcription, VZV microarrays using 75-base oligomers to 71 VZV open reading frames (ORFs) were designed and validated. The long-oligonucleotide approach maximizes the stringency of detection and polarity of gene expression. To optimize sensitivity, microarrays were hybridized to target RNA and the extent of hybridization measured using resonance light scattering. Microarray data were normalized to a subset of invariant ranked host-encoded positive-control genes and the data subjected to robust formal statistical analysis. The programme of viral gene expression was determined for VZV (Dumas strain)-infected MeWo cells and SVG cells (an immortalized human astrocyte cell line) 72 h post-infection. Marked quantitative and qualitative differences in the viral transcriptome were observed between the two different cell types using the Dumas laboratory-adapted strain. Oligonucleotide-based VZV arrays have considerable promise as a valuable tool in the analysis of viral gene transcription during both lytic and latent infections, and the observed heterogeneity in the global pattern of viral gene transcription may also have diagnostic potential.

Received 4 February 2005
Accepted 23 June 2005

INTRODUCTION

Varicella-zoster virus (VZV) is a neurotropic alpha herpesvirus that causes varicella (chicken pox) as a primary infection, and after a variable period of latency in the trigeminal and/or spinal ganglia, reactivates to produce herpes zoster (shingles) (Gilden *et al.*, 2000, 2003; Kennedy, 2002). The most significant neurologic complication of zoster is post-herpetic neuralgia (PHN), which affects almost half of individuals with zoster over the age of 50 years, and is highly refractory to treatment (Cohrs *et al.*, 2004; Gilden *et al.*, 2003). The experimental approach to VZV infection has been considerably limited by the highly cell-associated nature of the virus and the lack of an animal model in which VZV can be reactivated (Cohrs *et al.*, 2004).

A detailed analysis of viral transcription both *in vitro* and *in vivo* is important in terms of understanding the biology of VZV, including viral latency, and in the identification of potential viral targets that can be exploited therapeutically (Cohrs *et al.*, 1994, 1995, 1996, 1998, 2003a, b; Kennedy *et al.*, 1998, 2000). The development of gene microarray technology in which the entire viral transcriptome can be determined during infection has added a new dimension to such studies. A PCR-based VZV array system using predicted viral open reading frames (ORFs) has recently identified highly expressed viral genes during acute lytic infection (Cohrs *et al.*, 2003b), and we have previously described the use of long-oligonucleotide arrays in analysing global viral gene transcription during infection by alpha, beta and gamma members of the herpesvirus family (Chambers *et al.*, 1999; Ebrahimi *et al.*, 2003; Stingley *et al.*, 2000; Wagner *et al.*, 2002). Here we report the construction and validation of a novel VZV oligonucleotide microarray system, and show that it can be used to detect differences in the viral transcriptome in different cell types.

A list of VZV PCR primers is shown in Supplementary Table S1, a summary of RT-PCR results in MeWo and SVG cells in Supplementary Table S2, *in situ* hybridization using DIG-labelled probes to VZV gene 63 in VZV-infected MeWo and SVG cells at 72 h post-infection in Supplementary Fig. S1, and gels of RT-PCR experiments for VZV genes 31 and 61 in Supplementary Figs S2 and S3, available as supplementary material in JGV Online.

METHODS

Probe design and array fabrication. Probes were designed using the Oligo 6 primer design software (Molecular Biology Insights,

Table 1. VZV microarray probes

Oligonucleotide probes (75-mer) were designed based on the Dumas strain (Genbank accession no. X04370).

Gene	Start	End	Strand	Sequence (5′–3′)	Position
ORF1	915	592	−	CGTTCAAACAAGACCACCGGCGGTTCTTATTCCACTGGTTGATGTCCCAAGGCCACGATCCCGGAGAAAGGCGTC	732
ORF1	915	592	−	ACTCGTCGTTCAAACAAGACCACCGGCGGTTCTTATTCCACTGGTTGATGTCCCAAGGCCACGATCCCGGAGAAA	738
ORF2	1134	1847	+	TGGTGAAGCCGCACTTACCACGTCAGACCGACCCACTCTCCCAACCCTAACAGCCCAAGGAAGACCAACAGTTTC	1862
ORF2	1134	1847	+	TAACATGCAACTTGACAGAAGACTCTGGTGAAGCCGCACTTACCACGTCAGACCGACCCACTCTCCCAACCCTAA	1657
ORF3	2447	1911	−	GTCCGGACAGCTGGGTGTACATCTGGCGGCTATTGGGTATCACTGTCATTGTAAATCCCCCTTCTCGGCGGAGTG	1994
ORF4	4141	2788	−	GGAAGTCACCGATTGGGCAAATGATGAAGCTATTGGCTCCACTCCAGGCGAGGACTCCACAACGTCTAGAACTGT	3969
ORF4	4141	2786	−	TGTATTACCCGATTCAAACCATCATGGAGGAAGAGACGTGGAGACTGGATATGCACGCATCGAACGGGGACATCG	3799
ORF5	5274	4255	−	CCATGCGCGTTATTATACCCCACATACATTCGGATTCTGGCCTGGGTTGTTGTATGCACGCTCGCTATAGTAGAG	4483
ORF6	8577	5329	−	TGCCCATTACGAACGTCAAGTATTGGCTGCATATCGACGACTCTACTGGGGGTATGGATGCTCGCCGTTTTGGTA	7901
ORF7	8607	9383	+	AAACGTATCCGACAGAAACTCTTCAGCCCGTGTTGACCCCAAAACAGACGCAAGATGTACAACGCACAACCCCCG	9280
ORF8	10667	9480	−	CGTGTGTCCAACGGCATGGCCTGCAGGAGAACACTGTAAATTCTACGTATATAATCTCACGGGTGATGACATACG	9727
ORF9	11009	11914	+	CGACCCCTCGCGTACATCAACCAAACGACTCCAGCGGATCGGAAGATGACTTTGAAGACATCGATGAAGTAGTGG	11220
ORF10	12160	13389	+	CAGCGTCTGCCTTGAGGGAAATAAATTACCGCCGCCGAGAACTGGGACTGCCTCTAGTTAGATGTGGTCTTGTTG	13034
ORF11	13590	16046	+	AGGAGGACGCGATCGACGACGAGGGAGAGGCGGAGGAGGATTATTTTTCTGTAAGTCAAGTTTGCAGTCGAGACG	14230
ORF11	13590	16046	+	ATTGGAGACCATCTATCCCCGAGAACAGCCCATTCCCTCCGTGGACCTAGCCGAAAATCTTATGCAATACAGGAA	15917
ORF12	16214	18196	+	GCGCGCGTCTGTTATTCCAGATGATTTGCTTAGACGACATTTAAAAACGGGTCCTGCGGTCTCAGCGGGCACAGG	17044
ORF13	18441	19343	+	GAGATCGGGGGATATGGGCCTTGGGGTACCGTTCAACATTGCTGGATATGCACTTCTTACCTACATAGTAGCGCA	19046
ORF13	18441	19343	+	GCAAACGGTGAATTATCCTGCCAAGTATACCAGAGATCGGGGGATATGGGCCTTGGGGTACCGTTCAACATTGCT	19014
ORF14	21113	19434	−	GTCCAACATCGGAACTCGACGGACCTATCACCTATTCGTGTCATCTAGATGGTTACCCTAAAAAATTCCCTCCGT	19574
ORF15	22478	21261	−	CGTCTGCGAAGCTGCCGTCAATGCAACTATTATGGGGTTGATCGTCGTTTCGGGGTTATGGCCAACATCCGTGAA	22204
ORF16	23794	22571	−	GGAAACTCCCCGAAACCACATGGCAGGAGGGAATCGGAATTCGCGAATATTGTGTGGCTCCTCCAGTGGACCCTG	22630
ORF17	24149	25513	+	CCGTTTCCAAATATGCATCTAACCGATCGGAGGTGACAGTAGACGCCAGTTGGGCTTTAAACCTTCTGCCACCCT	25182
ORF18	26493	25576	−	GCGCGGACAGGCTTTTATCAGCGATTAATGTACCAAAACTATTTAACACCCCACCTCCCGATTCGGACTTTCCAC	25659
ORF19	28845	26521	−	CGGGGTCCTGGCGGCTGGGAACTTTCCATGTAAAAAATCATGTAAAGGTGTAAAAAACAACCGATCACTTGGCAT	27335
ORF20	30475	29027	−	TATAACCGCCGTGGCCAAAGGTCCCCAAGAAGCTGCACGTACAGACAAAACTTCAACTCGCAGGGTCACAGCCAA	29583
ORF21	30759	33872	+	CAAGGCAGCAGTTTCATTCGTTATGGACTCCAGGCAACAGTTTATTGTGGATTCTGGACCTCAGATGGGCGCGGT	33590
ORF22	34083	42371	+	GCCAAACTTTCCGCGGGACGTACACACATGGGGCGTATCTTCTAACCCGTTTAACTCACCGAACAGAGACCTATA	41993
ORF23	43138	42434	−	TCCGTTGGACAACAGCAACACGTGGTGTCGGGGTCTTCTGGACAACAACCGCAACAGGGAGCACAGTCAAGCACT	42581
ORF24	44021	43215	−	CCTGCGTTACCCGATACCCAAACTACGCGTGTCTGGAAACTTGCTCTACCCGTAGCTAACGTGACATATGCCCTG	43266
ORF25	44618	44151	−	GGAACACCATCCGGAATTAGAAGATGTATTTTCGGAGAATACGGGCGATTCGAATCCATCCATGGGTTCTTCTGA	44521
ORF25	44618	44151	−	AAGTAACGATTCAGAAAAATCTGCTTATGTTGTTCCATGTGAACATAGTGCCAGCGTGACCCGTCGCCGTGAACG	44206
ORF26	44506	46260	+	CGAGCGAGGATGCCTGTCCCGAAGTAGCATTTGGGCCTATTTTGTTAACTACCTTAAAAAACGCAAAGTGCCGTG	45635
ORF27	46127	47125	+	GTCGGGGGTATAAAATAGTCGCACACGTTTGGCAGACAACATTTTTACTGTCGGTATGTCGCAACCCAGAACAAC	46917
ORF28	50636	47055	−	TGGGGAAGCAAAGCGTAAGTTAATAATATCTGACTTAGCGGAAGATCCCATTCACGTAACATCACACGGGCTGTC	47350
ORF29	50857	54468	+	TTTGATCGCACTCGCCGTTTTATAATAGCATGTCCTAGAGGAGGTTTTATCTGCCCCGTAACAGGTCCCTCGTCG	53911
ORF30	54651	56960	+	GGCGGTGTCGTTGGTTCCAACTGGCTTCTCAGTCCATTTAGGGGCTTTTATTGCTTTTCTGGGGTAGAAGGCGTT	56538
ORF31	57008	59611	+	CCGACTCGAAATACCAGATCCCGACGAAGCGTGCCAGTTGAGTTGCGTGCCAATAGAACAATAACAACCACCTCA	58274
ORF32	59766	60194	+	CCTTAACCGCGACAGCCAATACGACTACTTAAACACATGTCCAGGGGGCCGTCATATTTCACTGGCACTGGAGAT	59993
ORF33	62138	60324	−	CAGTTGTGTAGGAACGACAGCGATATGGCTTCTGTAGCAGGTAACGCTAGTAATATCTCACCACAGCCCCCGTCG	61179
ORF34	63910	62174	−	AGGGGCAATAACTCTCCAGGGATTGTTTTCGGGCCATGGTATCGTACTCTGCAGGAACGGCTTGTGTTAGATAGG	63350

Table 1. cont.

Gene	Start	End	Strand	Sequence (5′–3′)	Position
ORF35	64753	63980	−	AGCTGAGGGATACCATGGCTTTAATAAAGGAAACCACACCCACGGGATCTGATGAAATAATGGTGACCCCCCTCC	64315
ORF36	64807	65829	+	CATGTCTCCGTTCGTATTATCGTTAGAACAGACACCCCAGCATGCGGCACAAGAACTAAAAACTCTGCTACCCCA	65676
ORF37	66074	68596	+	CGTTGTTTATTTAAGCAGGGATACTTGCGTGTCTGAACATGGTGTCATAGAGACGGTCGCACTGCCCCATCCGGA	68155
ORF38	70293	68671	−	ACGGAAAGGCATGAGTATGAGATATCCCGGTACTTAGATACCCTGTACTCTGGAGACCCCTGCTATAACGGCGCT	68848
ORF39	70633	71253	+	GCGTCTCGGAACAGACAAAGGACTTGCTTAGCGTTATGGTTAACCAGCACCCCGAAGAGGACGCAAAAGTGTGTA	70652
ORF40	71540	75727	+	GCGGAGGTTAACACTAATTGTAATACACTGGATCGGCTTCTAATGGAGGCAAAGGCTGTGGCGTCGCAAAGCTCC	75434
ORF41	75847	76794	+	GTGGATATAGCGCTGTCGTCATATTACATTAACGGTGCTCCACCAGACACGCTCTCGCTGTTAGAGGCATACCGA	75973
ORF42	78038	76854	−	TGGCACGTCTTCCAGTGAGATAGGGCGTTGCGTTACTCAATGCTTAGGCCACATACTCGCTTTACACCCCAATAC	77344
ORF45	82593	81538	−	TATTCCACTGTTCTCGGCTACTGCTCGACGGGCAATGTTTGGCGCGTTTCTATCGTCAACAGGGTACAACTGTAC	82280
ORF43	78170	80197	+	GGATGCGTTTTATAACAGCTCCTTGATGTATGCGGTTTTGGCGTATCTGTCATCTGTATATACACGACCACAAGG	79714
ORF44	80360	81448	+	CCCGCGGCTTCCGAAAAATCCATACGCATGTAAAGTTATTTCTCCGGGAGTGTGGTGGTCAGACGAACGAAGGCG	80854
ORF46	82719	83315	+	TTTGCGTTCCCACCACAATACCGACGGACATGAACCAAATGCAACCGCAGCCGATCAGCAAGAACGAGAATCCAC	83221
ORF46	82719	83315	+	GACCCTCGATCTAATCCGTGGGGGTGCGAGTGTACAAGATCCAGCATTTGTGTATGCCTTTACTGCTGCAAAAGA	82811
ORF47	83168	84697	+	CATTGGGCCAAGCACTCTTAGAAGTTATCCTGCTAGGACGTCTTCCCGGACAACTGCCCATTTCAGTACATCGGA	84261
ORF48	84667	86319	+	GCGATTACATCAGCATTGCGGTCATTGCGATGGGACAATCTTCATCCAGCGGTCGAGGAGGAATCTGTGGATTGT	86197
ORF48	84667	86319	+	CCTATGTATTATCCGGTTACTTTCCAGCGCTAAAACTACGGCCCTTCCTTGTCACCTTTATAGGACGTGTGCGCC	85949
ORF49	86226	86468	+	ATGTAACAGAGGACGCCGATAAATCCACACAACGCCGCCCACGAGTGATCGATGTAACACCAAAACGAAAACCTT	86359
ORF50	87882	86557	−	CCGCACAAATTACCCATCACAAGGCTACGGCTACGTCTATGAAAATGACTCAACATATGAAACGGACCGCGAGGA	86615
ORF50	87882	86578	−	TGGGAACGCTCGTGGCCTGTGCTACGTTGGGAACCGCCGCGCACTCGTATATGGACCGATTATATGACCCTATAT	86908
ORF51	87881	90385	+	CTGCATGTCGTACCTACCGCCAGTTGTATAACCTGCTTATGAGCCAGCGCCATTCGTTCTCTCAACAGCGTTACA	90156
ORF52	90493	92805	+	CCATCGTGTGCCTGTATTCCCCCCATAGACTGCGCTGCTCATCTCAAGCCCCTTATACACACGTTTGTCACTATT	92638
ORF53	93850	92858	−	CCCCCCTGTCCAGATGGTGTGGTGCAAGTACCCCCGGGATTGTTAAATGGACCTTTACGAGATTCGGAATATCAG	92954
ORF54	95984	93678	−	TTATATGAAATGCAGGTTCGCGCAGAGGTAATAAAACGGGGCCCACGGAGAACACCAAGTCCTTCCTGGGGTTTG	93987
ORF55	95996	98638	+	AGCCATGACAATTGCACGCTCACAGGGTCTGAGTTTAGAGAAGGTAGCTATCTGTTTTACGGCGGATAAACTGCG	98410
ORF56	98568	99299	+	ACGGTTTACGGGTAAACAGACCTGACGATCAGACCACACCAACACCAACCCCGCACCAGTATACATCGCAAAGGC	99127
ORF57	99626	99414	−	TGTACGCGAGTTAATTTTGTCGGGACACAACAACGTCGTATTACAGACATACACTGGTAAATGGTCAGACTGCCG	99484
ORF58	100272	99610	−	GAGCCTGCAAATGTTTGTGTTGTGTCAAAAAACCCATGCACCCCGTGTCAGAAACCTACTGTACGAGAGTATTCG	99785
ORF59	101219	100305	−	TGTGGGGTGCGCATGCACAGAAGACAACCCAACCGAATTCAAGATGTCATCTGGTGCTAACACACGCGCATCCGT	100406
ORF60	101649	101173	−	CGGGGACATACGCGATGCTTTGTTGGATGCCCTTTCCGGTGTATGGGTAGACTCTACTCCATCTTCCACAAATAT	101228
ORF61	104485	103085	−	AAGACCAGAAACCACCTCAACCGGGGAGACCTCTCGTGGCGATGAAAGGGATACCCGATTGGTAAATACACCCCA	103377
ORF62	109133	105204	−	GCTCGTATCGAGACTGCGTTTGCCAACCTGTACCCGGGCGAACAACCCCTGTGTTTGTGCCGCGGTGGGAACGTC	106032
ORF62	109133	105204	−	ATAGCATGGCTCCAGAACCCCAAGCTGACCGGTGTCAACTCGGCCCTGAACCAGTTCTACCAAAAGCTGTTGCCA	107499
ORF63	110581	111414	+	TTTGCATAGGAGCGCACTGGAATGTGACGTATCTGATGATGGTGGTGAAGACGATAGCGACGATGATGGGTCTAC	111018
ORF64	111565	112104	+	GAATTATATGACCGCCCCGGGGGAATTTGTCACAGGCTTTTTGACGCGTACCTGGGCTGCGGGTCCCTTGGAGTC	12099
ORF65	112640	112335	−	CGTTCGGCTGAAAAGTGTTATTATAGTGATAGCGAAAATGAAACGGCAGATGAATTTTTGCGTCGAATTGGAAAA	112455
ORF66	113037	114215	+	CGGCCACCGAGGCAACCGTGTTAAGAGCGTTAACCCACCCATCCGTTGTACAGCTTAAAGGAACGTTTACGTATA	113422
ORF67	114496	115558	+	CCAAATACAAAAACAAGAAGGGGCATACAAAATGCGACACCAGAATCCGATGTGATGTTGGAGGCCGCCATTGCA	115423
ORF68	115808	117676	+	CCCAACGCACCCCAATGCCTCTCTCATATGAATTCCGGTTGTACATTTACCTCGCCACATTTAGCCCAGCGTGTT	117005
ORF69	118332	117793	−	GCCCGATAATAAATGCATCCGCGCCGAATTATATGACCGCCCCGGGGGAATTTGTCACAGGCTTTTTGACGCGTA	117839
ORF70	119316	118483	−	CATAGGAGCGCACTGGAATGTGACGTATCTGATGATGGTGGTGAAGACGATAGCGACGATGATGGGTCTACGCCA	118801
ORF71	120764	124693	+	GGGAGATCCGGCTAGACAGTACCGCGCGCTGATTAACCTGATCTACTGTCCAGACAGAGACCCTATAGCATGGCT	122320

http://www.oligo.net/contact.htm). ORF- and strand-specific viral probe sequences were based on the original sequencing data (Davison & Scott, 1986), in which 71 ORFs, located on both strands (Dumas strain), were identified (Table 1), Genbank accession no. X04370. Design parameters for probe selection included: 75 base length, 85–95 °C melting temperature, 145–111 kcal mol^{-1} (607–465 kJ mol^{-1}) ΔG, 45–55 % GC content, <1000 bases from 3′ end, <1·5 kcal mol^{-1} (<6·3 kJ mol^{-1}) loop ΔG. Control elements on the array included 10 probes for cellular housekeeping genes, 18 negative-control probes (unrelated *Arabidopsis thaliana* genes), and printing vehicle without nucleic acids (Table 2). Probes were synthesized by MWG-biotech, resuspended at 100 μM in printing buffer (final concentration of 150 mM phosphate, 0·01 % SDS) and robotically printed in triplicate using a Genomic Solutions MG2 arrayer (with 4× MicroSpot 2·5K split pins) onto γ-aminopropylsilane (GAPS) II-coated slides (Corning Inc.). Arrays were stored under nitrogen at room temperature prior to use.

Viruses and cell lines. MeWo cells (a human melanoma cell line) were grown in Gibco 1966 DMEM medium containing glutamine, non-essential amino acids, 10 % fetal calf serum (FCS) and gentamicin. A total of 3×10^6 MeWo cells were mixed with an equal number of MeWo cells infected with VZV (Dumas strain) and grown in T175 flasks. By 72 h a viral infection was achieved, but no plaque formation was seen with this strain on MeWo cells. The SVG cell line is a human astroglial cell line (Major *et al.*, 1985) and was a generous gift from Dr E. O. Major. VZV-infected cells and uninfected SVG cells infected with VZV were treated in a similar manner to MeWo cells, except that the medium used for SVG cells was MEM containing Earle's salt, glutamine, gentamicin and 10 % FCS. In addition, with the Dumas strain of virus, plaques are formed in SVG cells. To obtain the results reported below, a total of five 250 ml flasks of VZV-infected and five flasks of non-infected MeWo cells and SVG cells were harvested at 72 h when the observed cytopathic effects (CPEs) were maximal and similar in both cell types. The pooled data from these experiments were then statistically analysed to obtain the final results.

Isolation of RNA. RNA was extracted from cells using Qiagen RNeasy kits. Approximately 10^7 cells were trypsinized from the flasks and resuspended in lysis buffer containing β-mercaptoethanol. The samples were placed on a QIAshredder spin column and centrifuged

Table 2. Microarray probes for human housekeeping genes and negative controls

(a) Ten 75-mer oligonucleotide probes were designed for cellular transcripts. The array also included probes for (b) eighteen *Arabidopsis thaliana* genes.

Accession no.	Sequence (5′–3′)
(a)	
AJ000099	GTGACGCGGGGTACACCACAAGCACGGAGACCTGCCAGTACCTCAAAGATTACCTGACACGGCTGCTGGTCCCCT
D84361	AAGGACAGAGTCTTTGACAGTATCAGCCACCTCATCAACCACCACCTAGAAAGCAGCCTGCCCATTGTCTCTGCA
J04038	AACATGGAAGAAGCTATTCTGTGGGCAGCCCCAGGGAGGCTGACAGGTGGAGGAAGTCAGGGCTCGCACTGGGCT
J04617	AATAGGTCGCTTTGCTGTTCGTGATATGAGACAGACAGTTGCGGTGGGTGTCATCAAAGCAGTGGACAAGAAGGC
K00558.1	CCGTGAAGATATGGCTGCCCTTGAGAAGGATTATGAGGAGGTTGGTGTGGATTCTGTTGAAGGAGAGGGTGAGGA
M60854	AGGAGCGATTTGCTGGTGTAGACATCCGTGTCCGTGTAAAGGGTGGTGGTCACGTGGCCCAGATTTATGCTATCC
U02629	CCGCATGGTGCTGAATGGCTGAGGACCTTCCCAGTCTCCCCAGAGTCCGTGCCTTTCCCTGTGTGAATTTTGTAT
X00351	CCCCAAGGCCAACCGCGAGAAGATGACCCAGATCATGTTTGAGACCTTCAACACCCCAGCCATGTACGTTGCTAT
X58536	CGTGTCCACCGTGACCCCTGTCCCCACACTGACCTGTGTTCCCTCCCCGATCATCTTTCCTGTTCCAGAGAAGTG
Z12962	TCGCCCTCTGATCGCCGATCACCTCTGAGACCCACCTTGCTCATAAACAAAATGCCCATGTTGGTCCTCTGCCCT
(b)	
AY045834	AATAAGTATAGGTCTTGGTCCTTCGGGGGAGCTTAGATATCCTGCACATCCTTCTGGAGATGGGAGGTGGAAATT
AY062116	ATTTACCTGTTGAAGAGAAAGCTGAGCTCAATTCTTTGCAGAGAGGCAGCAGGCTTGTAGCTTCCGGTTATGTGC
M90394.1	CCTAGGTCCTAAGTCTTTTTACTTGCAACCAAAGGGCATTTTGGTCGTTTTTTAAGTTTCATGGACCAGATATGC
U09332.1	AAGAGAAGGTACCTCCGGTGGTGGTTGCGGAGATGACCTTGACATCACTCTAGATAGATCTTCCTCACGTGGAAC
U91966.1	TCTATCTGGTGGAGATCATATTCACGCGGGTACAGTAGTAGGTAAACTTGAAGGAGACAGGGAGTCAACTTTGGG
X14212.1	CGTATGGGTGGTACTACTCAGTACACTGTCAACAACCAGATGGTTAACGCAACACTCATGAACATTGCTGATAAC
X56062.1	CTTCTCTCTTCTTCCAAGTCTAAATTCGTATCCGCCGGAGTTCCACTCCCAAACGCCGGGAATGTTGGTCGTATC
X68145.1	GACCTTCAAAGATCACAGTACTCTCAATCCGAAGCAGAAGCAAGCATTGGCTAAACAATTAGGGTTACGAGCAAG
AF159801*	SR4_LTP4
AF159803*	SR5_LTP6
AF168390*	SR7_RCP1
AF191028*	SR6_XCP2
AF198054*	SR8_NAC1
AF247559*	SR9_TIM
U91966*	SR3_rbcL
X14212*	SR2_RCA
X56062*	SR1_CAB
X58149*	SR10_PRKase

*Stratagene 'SpotReport Oligo Array Validation System' proprietary sequences (catalogue no. 252170).

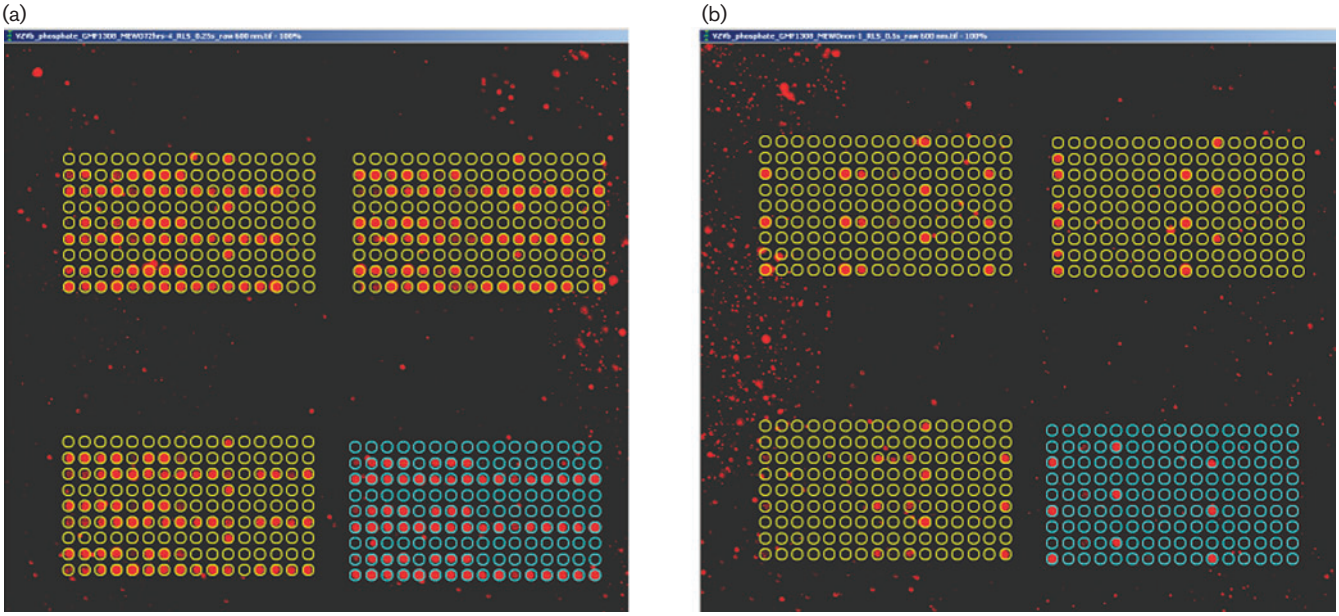

Fig. 1. Typical QUANTARRAY (Packard Biosciences) image with grid overlay of (a) MeWo cells infected with Dumas strain for 72 h and (b) uninfected MeWo cells.

at maximum speed for 2 min. An equal volume of 70 % ethanol was added to the flow-through which was placed on the Qiagen column, washed and then DNase (Qiagen RNase-free DNase) was added to the column. After several washes, the RNA was eluted and it was usually necessary to DNase-treat again (DNA-free kit, Ambion). The absence of residual DNA was shown by PCR for β-actin. RT-PCR was performed on all samples, and as a further check for DNA contamination, PCR was also performed on samples which were not reverse transcribed. RT-PCR also provided a validation for the presence of VZV-specific RNAs. Primers for VZV genes 37 (late, L), 28 (early, E) and 63 (immediate early, IE), as well as 62 (IE), 10 (L), 31 (L) and 4 (IE) were used, as well as nested primers for genes 63 and 62 (refer to Supplementary Table S1 for all VZV PCR primers used in this study). All of these VZV genes could be detected by RT-PCR (gels of RT-PCR experiments for VZV genes 31 and 61 are shown in Supplementary Figs S2 and S3).

The total RNA samples were quality-control checked on 2100 Bioanalyser NanoChips (Agilent) and a BioMate 5 UV spectrophotometer (Thermo Spectronic).

Array hybridization. Biotin [-dUTP (50 nmol), Roche Diagnostics] -labelled cDNA was synthesized from 2·5 μg total RNA, as specified by the manufacturer (Protocol for Direct Labelling for cDNA with Biotin-dUTP, Qiagen). The biotinylated target cDNAs were hybridized to the arrays (18 h at 42 °C), washed, HiLight Resonance Light Gold Particle hybridized (1 h at room temperature) and washed, as specified by the manufacturer (HiLight Array Detection Protocols – For Single-Colour Detection on the HiLight Reader using Resonance Light Scattering, Qiagen).

Data processing and statistical analysis. Array hybridization and analysis followed standard operating procedures, as described by Forster *et al.* (2003). Array data can be accessed at the MIAME-compliant database GPX, accession no. GXE-00039 (http://www.gti.ed.ac.uk/GPX/).

Image quantification. QUANTARRAY (Packard Biosciences) image analysis software (with 'histogram quantification' correction) was used for initial data capture. A typical hybridization image is shown in Fig. 1. To define the linear dynamic range of the biotin–gold particle light scatter and to control for scanning parameters (exposure time of the white-light source), arrays were scanned at five increasing exposure times, thereby initially generating five datasets per array. These datasets were then analysed against each other by scatter plots. The scan with the highest linear range of expression but no genes saturated at the 16-bit scan limits (maximum intensity value = 65535) was chosen as the dataset best representing an array.

Noise correction. Any localized array background variation was corrected for by subtracting the individual background intensity from the expression value for each gene.

Print quality correction. Triplicate printing of each probe on an array allowed us to compute the median expression value of each such triplicate as the representative value for this gene.

Array quality control. Receiver-operating-characteristics (ROC) analysis was performed for each array hybridization in the study. Sets of known positive- (n = 30) and negative-control probes (n = 156, including unused spike controls) on the chip represented the 'gold standard', against which the expression values were compared. The area under curve (AUC) was calculated for each array. Clear distinction (AUC close to 1) of positive and negative controls was taken to be an indicator of array/hybridization quality, since a high value meant that the expression values for known positive- and negative-control probes did not overlap. An AUC close to 0·5 would indicate that there is no expression-level cut-off that can clearly distinguish between positive and negative signals. As a consequence, one biological replicate from the non-infected MeWo cell line was withdrawn from analysis.

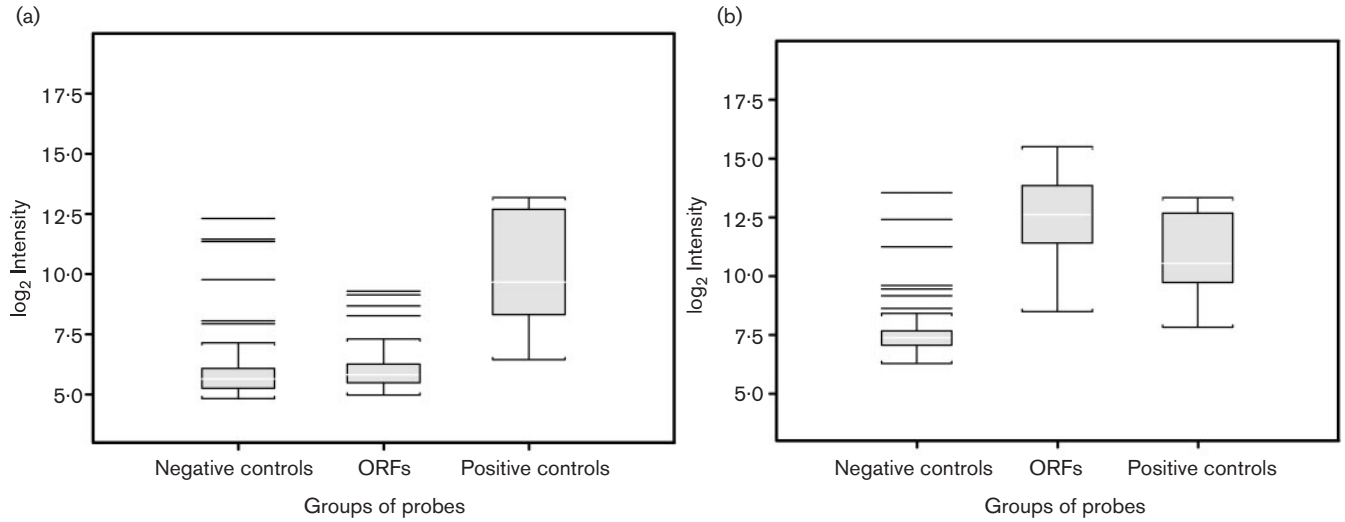

Fig. 2. Box-and-whiskers plots of VZV microarray validation. All spotted probes were placed into three groups (negative controls, ORFs and positive controls) to visualize their overall log-transformed signal intensities. The median value is represented by the line inside the box. Above this line are data in the third quartile and below this line are data in the first quartile. (a) MeWo non-infected (the outlying probes in the ORFs group are ORFs 10, 59, 60 and 63); (b) MeWo 72 h infected (Dumas strain).

Data transformation. Following the above, for further processing, the $\log_2$ of all data was obtained.

Normalization. The chosen method was scaling of the array medians to a common reference value by adding a correctional constant (Forster *et al.*, 2003). Normalization estimates were based on a set of host-encoded housekeeping genes ($n=30$), because a global normalization method based on the distribution of all probes on the array is inappropriate for most targeted (i.e. genome subset) arrays. For a targeted array, it can be assumed that a large proportion of genes will change expression between uninfected and infected samples; any overall expression differences between different samples are therefore due to hybridization/scanning and to real biological differences. All 30 housekeeping spots were assessed for consistency by means of a k-means clustering on their raw expression values across all arrays. As a result of this, the most reliable and rank-invariant set was chosen as the normalization set ($n=12$) accounting for hybridization/scanning effects only. These are triplicate spots of probes representing major histocompatibility complex 1 (MHC1), α-tubulin, glyceraldehyde-3-phosphate deydrogenase (GAPDH) and myosin light chain (alkali) Alt. Splice2.

Measurement thresholding. Subsequent to normalization, the lower threshold for reliable measurement of gene-expression values was computed as the 80th percentile of signal intensities of the *Arabidopsis thaliana* negative controls ($n=18\times3$). This threshold level was used to determine whether a signal was above the detection error associated with each individual array. The threshold level value was subtracted from the expression value for each ORF. In tables and figures, a value lower than 0 is represented as a 1.

Inference analysis. Statistical comparisons were performed for each gene to determine the significance of differential expression between infected and uninfected samples. The statistical sample size was $n=5$ independent biological samples per group, except for the MeWo non-infected group, for which $n=4$ (see Methods). Although sufficient for the computation of test statistics, a per-condition sample size of five limited the direct biological interpretability of results without laboratory validation. However, this study did include RT-PCR measurements as a means of validating the microarray results. Interpretation of results was done on the premise that the significance tests serve as a valid 'interest filter'. To make optimum use of the microarray platform and the given sample sizes, the method of analysis was a permutation of Welch's t test performed on $\log_2$-transformed data. A Westfall and Young step-down adjustment was used on the resulting P values to correct for problems created by testing multiple genes simultaneously.

RESULTS AND DISUSSION

In the present study, a total of 40 chip hybridizations were analysed. The collective results can be used in conjunction with probe classification to assess the overall validity of the microarray approach. Data on signal values of the grouped array data are shown in Fig. 2 as a box-and-whiskers plot for each of the classes of gene probes on the array: negative controls, ORFs and positive controls. A comparison of uninfected with infected samples led to the development of a response profile that highlights the whole-scale expression of viral transcription at 72 h, whereas the cellular and negative probes remain by and large unaffected. The plots give a numerical and statistical representation of the response profile of the probe sets, and thereby provide validation data for the VZV arrays, in which all probe classes behaved as expected. The comparative analysis has been performed after using a set of invariant housekeeping genes in a form of 'subset' normalization, as a reference point for the various respective samples.

To evaluate the sensitivity and specificity of the VZV microarrays in a quantitative manner, ROC analysis was

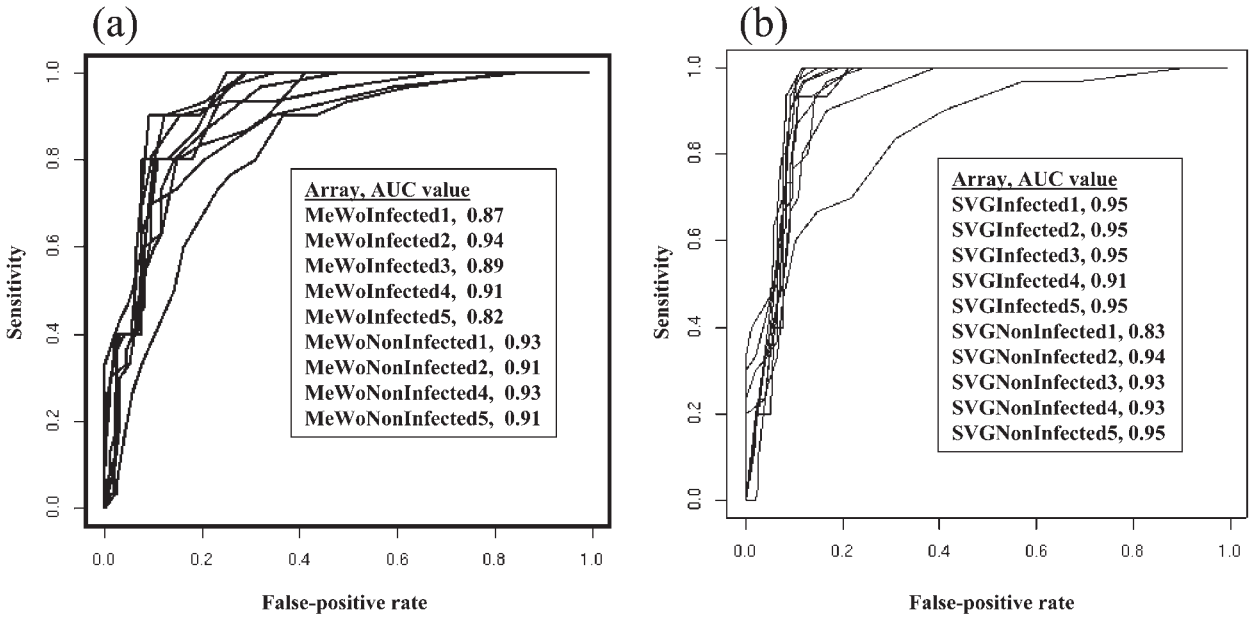

Fig. 3. Quality control by ROC analysis. One ROC analysis was performed for each array hybridization in the study. This is a representative graph containing all ROC curves for (a) MeWo and (b) SVG non-infected and infected at 72 h arrays. Sets of known positive- ($n=30$) and known negative-control probes ($n=156$) represent the 'gold standard' against which expression values are compared. An AUC of each array is shown.

performed for each array hybridization in the study (see Methods). Fig. 3 shows a representative graph containing all array hybridization ROC curves for non-infected and infected MeWo and SVG at 72 h. An AUC of 1 implies no overlap in expression values between negative and positive controls, whereas an AUC of 0·5 indicates the negative and positive probes are not distinguishable by their expression values. The mean AUC value for all tissue-culture experiments was 0·92. VZV infection of clinically obtained cell culture samples (ROC not shown) yielded a mean AUC of 0·81. As expected, variation is evident between replicate samples, which underscores the statistical use of replication in array experiments.

Unlike other members of the herpesvirus family, VZV is particularly difficult to grow in culture. Accordingly, infections are limited to virus-infected cell-passaged stocks, and quantification of virus is far more difficult than is the case with herpes simplex virus (HSV). In addition, unlike other alpha herpes viruses, such as HSV, it would be very difficult to synchronize the infection of cells with VZV. Since Cohrs *et al.* (2003b) have shown that the relative expressions of the transcripts are similar at different time points, we focused on the time of maximum CPE and extended their results by comparing the transcriptomal pattern in two different cell lines: MeWo, a human melanoma cell line, and SVG, a human astroglial cell line. The first array experiments were carried out on virally infected MeWo cells, one of the most permissive cell types for VZV replication. The accumulated results for these experiments at 72 h using the laboratory Dumas VZV strain are shown in detail in Table 3. There was a highly significant detection of the expression of 68/71 viral genes. The greatest expression detected was that of ORF 57, followed by (in order of extent of expression) ORFs 9, 49, 58, 48 and 69. The only ORFs whose expression was not significant were 6, 22 and 56.

When the transcriptional profile of the Dumas VZV strain in SVG cells at 72 h was studied, the results showed a marked contrast to those observed in MeWo cells. The accumulated results in SVG cells are shown in detail in Table 4. Only 20/71 VZV ORFs showed a highly significant expression in infected SVG cells, with the greatest expression observed for ORFs 24, 68, 61, 13, 32 and 53. A comparison of the highly significant signal intensities of the viral genes in MeWo cells compared with the signal intensities of the same genes in SVG cells at the same time-period is shown in Table 5, which also lists the known or putative functions of those ORFs. The only ORFs in the 'top six' expressed genes in MeWo cells that were also expressed in SVG cells were 49, 57 and 58. However, none of the top six expressed genes in MeWo cells can be found in the top six expressed genes in the SVG cells after viral infection. Analysis of the intensity ratio between the mean of the top 20 % expressed viral genes compared with the mean of the invariant cellular genes indicated similar ratios of between 1 : 1 and 1 : 1·5 in SVG and MeWo cells, respectively. These results showed clearly that the infected cell type strongly influences the VZV transcriptome, which likely relates to the state of permissiveness of the cellular system. It was obviously important to study MeWo and SVG cells that had an equivalent level of infection at 72 h, as otherwise any detected differences seen

Table 3. Fold change of signal intensities for the viral transcripts of VZV Dumas-infected (72 h post-infection) MeWo cells and non-infected MeWo cells

The table also contains significance *P* values. **, *P* value $< 0{\cdot}05$. The fold changes are from absent to present. Zero signal intensities were therefore given an arbitary value of 1 before the fold changes were calculated.

ORF	Fold change for infected (72 h Dumas) versus uninfected MeWo cells (standard error)	Westfall & Young *P* value
ORF01	8·88 (0·32)	**
ORF02	6·07 (0·36)	**
ORF03	7·45 (0·37)	**
ORF04	12·03 (0·38)	**
ORF05	5·08 (0·45)	**
ORF06	0 (0·43)	
ORF07	11·34 (0·34)	**
ORF08	10·10 (0·31)	**
ORF09	14·48 (0·41)	**
ORF10	4·63 (0·41)	**
ORF11	11·44 (0·36)	**
ORF12	10·24 (0·35)	**
ORF13	8·69 (0·37)	**
ORF14	11·54 (0·34)	**
ORF15	10·29 (0·33)	**
ORF16	9·29 (0·42)	**
ORF17	9·90 (0·43)	**
ORF18	12·30 (0·32)	**
ORF19	4·48 (0·35)	**
ORF20	10·47 (0·36)	**
ORF21	10·65 (0·44)	**
ORF22	6·77 (0·45)	
ORF23	13·82 (0·37)	**
ORF24	13·41 (0·41)	**
ORF25	10·50 (0·34)	**
ORF26	9·46 (0·34)	**
ORF27	11·15 (0·34)	**
ORF28	11·93 (0·34)	**
ORF29	11·97 (0·46)	**
ORF30	8·29 (0·46)	**
ORF31	10·50 (0·36)	**
ORF32	12·71 (0·39)	**
ORF33	13·05 (0·42)	**
ORF34	9·50 (0·38)	**
ORF35	8·19 (0·45)	**
ORF36	11·99 (0·49)	**
ORF37	12·98 (0·47)	**
ORF38	12·56 (0·39)	**
ORF39	8·91 (0·38)	**
ORF40	6·16 (0·36)	**
ORF41	12·81 (0·33)	**
ORF42	11·87 (0·31)	**
ORF43	9·29 (0·33)	**
ORF44	10·99 (0·37)	**
ORF45	5·75 (0·38)	**
ORF46	4·75 (0·46)	**
ORF47	11·36 (0·35)	**
ORF48	13·97 (0·48)	**
ORF49	14·32 (0·34)	**
ORF50	12·48 (0·34)	**
ORF51	10·10 (0·40)	**
ORF52	12·02 (0·40)	**
ORF53	12·73 (0·41)	**
ORF54	10·33 (0·46)	**
ORF55	8·60 (0·52)	**
ORF56	3·56 (0·48)	
ORF57	14·49 (0·44)	**
ORF58	14·26 (0·37)	**
ORF59	5·25 (0·38)	**
ORF60	3·54 (0·40)	**
ORF61	13·52 (0·37)	**
ORF62	7·16 (0·35)	**
ORF63	5·95 (0·39)	**
ORF64	9·48 (0·37)	**
ORF65	11·47 (0·36)	**
ORF66	10·24 (0·33)	**
ORF67	13·67 (0·34)	**
ORF68	10·44 (0·40)	**
ORF69	14·18 (0·37)	**
ORF70	13·64 (0·34)	**
ORF71	10·66 (0·31)	**

on the arrays might have been due to initial differences in infection levels. The level of infection in the two cell lines at 72 h was indeed comparable, with approximately 90 % of MeWo cells and 80 % of SVG cells infected, as assessed by the level of CPE and by *in situ* hybridization using a VZV gene probe (Supplementary Fig. S1).

It was also important to confirm the detection of specific VZV ORF expression on the arrays by a different method. We therefore used RT-PCR to examine the presence of a range of representative VZV genes (ORFs 4, 10, 28, 31, 37, 62 and 63) at 72 h after infection in both MeWo and SVG cells. While not all of these genes had been shown to be significantly expressed on the arrays in the two culture systems, we were able to detect the presence of all of these genes by RT-PCR (representative gels are shown in Supplementary Figs S2 and S3). We strongly suspect that this is due to the greater sensitivity of RT-PCR compared with microarrays, even though the latter have the considerable advantage of examining the expression of the entire VZV genome simultaneously. Evidence for this explanation was provided by our semi-quantitative arbitrary assessment of the intensity of the gel bands for representative VZV ORFs 31, 37, 61 and 62 in MeWo cells compared with SVG cells [see Supplementary Table S2, in which Quantity One 1-D analysis

Table 4. Fold change of signal intensities for the viral transcripts in VZV Dumas infected (72 h post-infection) SVG cells and non-infected SVG cells

The table also contains significance *P* values. **, *P* value $<0{\cdot}05$. The fold changes are from absent to present. Zero signal intensities were given an arbitary value of 1 before the fold changes were calculated.

ORF	Fold change for infected (72 h Dumas) versus uninfected MeWo cells (standard error)	Westfall & Young *P* value
ORF01	7·96 (0·68)	
ORF02	1·33 (0·54)	
ORF03	3·30 (0·63)	
ORF04	10·31 (0·54)	
ORF05	7·15 (0·95)	
ORF06	5·86 (0·66)	
ORF07	8·66 (0·43)	
ORF08	8·24 (0·74)	
ORF09	4·51 (0·76)	
ORF10	1·71 (0·84)	
ORF11	4·22 (0·81)	
ORF12	7·55 (0·58)	
ORF13	10·37 (0·72)	**
ORF14	7·54 (0·59)	
ORF15	8·60 (0·77)	
ORF16	6·45 (0·99)	
ORF17	7·67 (0·58)	
ORF18	9·69 (0·87)	**
ORF19	−0·27 (0·90)	
ORF20	9·46 (0·85)	**
ORF21	1·14 (0·90)	
ORF22	9·32 (0·63)	
ORF23	3·44 (0·61)	**
ORF24	11·09 (0·48)	**
ORF25	8·42 (0·59)	
ORF26	6·32 (0·74)	
ORF27	9·15 (0·56)	
ORF28	9·61 (0·55)	
ORF29	8·96 (0·74)	**
ORF30	7·64 (0·72)	
ORF31	7·81 (0·49)	
ORF32	10·41 (0·47)	**
ORF33	7·86 (0·67)	**
ORF34	6·70 (0·67)	
ORF35	5·40 (0·73)	
ORF36	9·53 (0·68)	
ORF37	5·02 (0·53)	**
ORF38	9·58 (0·55)	
ORF39	5·89 (0·57)	
ORF40	7·86 (0·45)	
ORF41	9·92 (0·89)	
ORF42	9·28 (1·17)	
ORF43	5·01 (0·66)	
ORF44	7·40 (0·53)	
ORF45	7·54 (0·60)	
ORF46	4·16 (0·64)	
ORF47	8·77 (0·68)	**
ORF48	3·68 (0·55)	
ORF49	3·42 (0·64)	**
ORF50	4·91 (0·56)	**
ORF51	7·53 (0·55)	
ORF52	7·35 (0·51)	
ORF53	9·88 (0·53)	**
ORF54	7·87 (0·86)	
ORF55	0·35 (0·89)	
ORF56	−0·38 (0·51)	
ORF57	4·93 (0·56)	**
ORF58	6·16 (0·54)	**
ORF59	0·81 (0·70)	
ORF60	0·45 (0·68)	
ORF61	10·80 (0·49)	**
ORF62	5·68 (0·49)	
ORF63	2·43 (0·43)	**
ORF64	3·47 (0·54)	**
ORF65	9·17 (0·73)	
ORF66	7·32 (0·62)	
ORF67	3·17 (0·52)	
ORF68	10·93 (0·63)	**
ORF69	4·21 (0·70)	
ORF70	5·10 (0·89)	**
ORF71	9·21 (1·04)	

software (Bio-Rad) was used]. While the signal intensity of the bands was always greater in MeWo than in SVG cells, the signals for ORF 61, which was expressed on arrays in both MeWo and SVG cells, were very similar in both cell types. However, the intensity of the bands for ORF 31, which was expressed on arrays in MeWo but not SVG cells, was higher in MeWo cells than in SVG cells.

The array design used probes with a high degree of biophysical and thermodynamic equivalence, and allowed the determination of both the stringency and polarity of viral gene expression. The latter was also quantified using robust statistical analyses. A comparison of our results with the recent study of Cohrs *et al.* (2003b) reveals that the transcription of some viral genes was significantly elevated in both systems. Thus, there was a striking detection of the transcription of VZV ORF 9 in MeWo cells infected with VZV, this gene being consistently highly transcribed in lytically infected cultures. This is the first independent confirmation of the finding of Cohrs *et al.* (2003b) that ORF 9 is the most highly expressed ORF in BSC-1 cells infected with the VZV Ellen laboratory strain. This protein is known to be an abundant tegument phosphoprotein, the protein being phosphorylated by the ORF 47-encoded protein kinase (Ng & Grose, 1992; Ng *et al.*, 1994), and then associating with phosphorylated IE 62 protein (Spengler

Table 5. Highly significant fold changes that are equivalently expressed between 72 h post-infection (Dumas strain) SVG cells and MeWo cells

The VZV ORFs in this table with assigned functions are 13, 18, 29, 33, 37, 47, 49, 61, 63/70 and 68. The rest are assumed functions.

ORF	Fold change infected versus uninfected SVG cells (standard error)	ORF function	Fold change infected versus uninfected MeWo cells (standard error)
ORF13	10·37 (0·72)	Thymidylate synthase	8·69 (0·37)
ORF18	9·69 (0·87)	Ribonucleotide reductase, small subunit	12·30 (0·32)
ORF20	9·46 (0·85)	Capsid protein	10·47 (0·36)
ORF23	3·44 (0·61)	Capsid protein	13·82 (0·37)
ORF24	11·09 (0·48)	Membrane-associated phosphoprotein	13·41 (0·41)
ORF29	8·96 (0·74)	ssDNA binding protein	11·97 (0·46)
ORF32	10·41 (0·47)	Hypothetical protein	12·71 (0·39)
ORF33	7·86 (0·67)	Protease	13·05 (0·42)
ORF37	5·02 (0·53)	Glycoprotein H	12·98 (0·47)
ORF47	8·77 (0·68)	Serine/threonine protein kinase	11·36 (0·35)
ORF49	3·42 (0·64)	Myristylated virion protein	14·32 (0·34)
ORF50	4·91 (0·56)	Glycoprotein M	12·48 (0·34)
ORF53	9·88 (0·53)	Hypothetical protein	12·73 (0·41)
ORF57	4·93 (0·56)	Hypothetical protein	14·49 (0·44)
ORF58	6·16 (0·54)	Nuclear phosphoprotein	14·26 (0·37)
ORF61	10·80 (0·49)	Transactivator	13·52 (0·37)
ORF63	2·43 (0·43)	Transactivator/transrepressor	5·95 (0·39)
ORF64	3·47 (0·54)	Virion protein	9·48 (0·37)
ORF68	10·93 (0·63)	Glycoprotein E	10·44 (0·40)
ORF70	5·10 (0·89)	Transactivator/transrepressor	13·64 (0·34)

et al., 2001). The oligonucleotide probes selected provide a global and simultaneous readout of VZV ORF transcriptional activity. In addition, transcriptional polarity is defined, since the probes are single stranded and of sense orientation. However, the probes were not designed to address the fine details of VZV transcriptional complexity. Indeed, a limitation of this approach is that the array probes do not allow for the differentiation of co-terminal and collinear transcripts, which is a feature of VZV transcription. In this respect, certain probes (e.g. for ORFs 4/5 and 63/64) probably detect multiple transcripts arising from the same strand.

The six most abundant VZV transcripts detected in MeWo cells infected by the laboratory-adapted Dumas VZV strain were ORFs 57, then 9, 49, 58, 48 and 69. Four of these ORFs were also in the top six transcribed genes in the study of Cohrs *et al.* (2003b), namely ORFs 9, 49, 57 and 69 (ORF 64 was highly expressed in the previous study, and ORFs 64 and 69 are duplicated genes). The HSV 1 homologue of the protein encoded by ORF 49 has been identified as a virion protein (MacLean *et al.*, 1989), while the protein encoded by ORF 57 is a hypothetical protein, which has yet to be identified but is dispensable for virus replication in cell culture (Cox *et al.*, 1998). ORF 33, which encodes a protease (McMillan *et al.*, 1997), was not significantly expressed in MeWo cells, despite being highly expressed in BSC-1 cells infected with VZV Ellen (Cohrs *et al.*, 2003b). ORF 64/69 encodes a 19·8 kDa protein which is dispensable for virus replication (Sommer *et al.*, 2001). Despite the not-unexpected differences, these transcriptional similarities between the two systems reinforce the reliability of microarray technology.

Both the cell type used for infection (MeWo versus BSC-1) and the strain of virus used (Dumas versus Ellen) were different in the Cohrs *et al.* (2003b) study and this study, and this is presumably a major contributing reason for the differences observed. In our study, the transcriptome of VZV Dumas strain on either the MeWo cells (known to be VZV-permissive) or SVG cells was analysed at 72 h and found to differ markedly, as shown in Table 5. Since the same virus was used in both cases, and the ratio between the top 20 % of viral and invariant cellular genes was equivalent, we conclude that the infected host-cell type influences the viral transcriptome. It is known that during acute VZV infection of cultured human astroglial cells, host-protein synthesis may be altered, as evidenced by the down-regulation of glial fibrillary acidic protein (GFAP) under these conditions (Kennedy *et al.*, 1994). Since SVG cells are also astroglial, it is possible that some form of host-cell modulation by the infection may have affected the virus–host cell interaction to produce the observed phenotype.

To date we, and others, have performed a large number of diverse microarray studies of herpesvirus family genomes, including the analysis of a wide range of different strains and mutant genomes (Chambers *et al.*, 1999; Ebrahimi *et al.*, 2003; Jenner *et al.*, 2001; Stingley *et al.*, 2000; Sun *et al.*, 2004; Wagner *et al.*, 2002; Yang *et al.*, 2002). Overall, these experiments reveal a marked robustness of the herpes viral transcription programme. A key property of robust systems is their general insensitivity to changes of internal parameters. We also have preliminary data (P. G. E. Kennedy and others, unpublished results), based on two different VZV patient isolates, that suggest that the viral RNA transcriptional signatures may differ markedly from patient to patient, but much further work will be required to determine whether this can be used as a potential correlate or predictor of the development of PHN. Both oligonucleotide- and PCR-based VZV arrays are very likely to prove powerful tools for the future investigation of viral gene function, and may also have diagnostic potential.

ACKNOWLEDGEMENTS

This work was supported by a grant to P. G. E. K. from the Chief Scientist's Office (CSO) of Scotland and in part from grants to P. G. from SHEFC and the Biotechnology and Biological Sciences Research Council (BBSRC). We also thank our colleagues at the SCGTI for advice and help and Professor Ed Wagner for his many valued contributions, including sharing data on the application of the light-scattering technique to viral microarrays.

REFERENCES

Chambers, J., Angulo, A., Amaratunga, D. & 9 other authors (1999). DNA microarrays of the complex human cytomegalovirus genome: profiling kinetic class with drug sensitivity of viral gene expression. *J Virol* **73**, 5757–5766.

Cohrs, R. J., Srock, K., Barbour, M. B., Owens, G., Mahalingam, R., Devlin, M. E., Wellish, M. & Gilden, D. H. (1994). Varicella-zoster virus (VZV) transcription during latency in human ganglia: construction of a cDNA library from latently infected human trigeminal ganglia and detection of a VZV transcript. *J Virol* **68**, 7900–7908.

Cohrs, R. J., Barbour, M. B., Mahalingam, R., Wellish, M. & Gilden, D. H. (1995). Varicella-zoster virus (VZV) transcription during latency in human ganglia: prevalence of VZV gene 21 transcripts in latently infected human ganglia. *J Virol* **69**, 2674–2678.

Cohrs, R. J., Barbour, M. & Gilden, D. H. (1996). Varicella-zoster virus (VZV) transcription during latency in human ganglia: detection of transcripts mapping to genes 21, 29, 62, and 63 in a cDNA library enriched for VZV RNA. *J Virol* **70**, 2789–2796.

Cohrs, R. J., Barbour, M. & Gilden, D. H. (1998). Varicella-zoster virus gene 21: transcriptional start site and promoter region. *J Virol* **72**, 42–47.

Cohrs, R. J., Gilden, D. H., Kinchington, P. R., Grinfeld, E. & Kennedy, P. G. E. (2003a). Varicella-zoster virus gene 66 transcription and translation in latently infected human ganglia. *J Virol* **77**, 6660–6665.

Cohrs, R. J., Hurley, M. P. & Gilden, D. H. (2003b). Array analysis of viral gene transcription during lytic infection of cells in tissue culture with varicella-zoster virus. *J Virol* **77**, 11718–11732.

Cohrs, R. J., Gilden, D. H. & Mahalingam, R. (2004). Varicella zoster virus latency, neurological disease and experimental models: an update. *Front Biosci* **9**, 751–762.

Cox, E., Reddy, S., Iofin, I. & Cohen, J. I. (1998). Varicella-zoster virus ORF57, unlike its pseudorabies virus UL3.5 homolog, is dispensable for viral replication in cell culture. *Virology* **250**, 205–209.

Davison, A. J. & Scott, J. E. (1986). The complete DNA sequence of varicella-zoster virus. *J Gen Virol* **67**, 1759–1816.

Ebrahimi, B., Dutia, B. M., Roberts, K. L. & 7 other authors (2003). Transcriptome profile of murine gammaherpesvirus-68 lytic infection. *J Gen Virol* **84**, 99–109.

Forster, T. D., Roy, R. & Ghazal, P. (2003). Experiments using microarray technology: limitations and standard operating procedures. *J Endocrinol* **178**, 195–204.

Gilden, D. H., Kleinschmidt-DeMasters, B. K., LaGuardia, J. J., Mahalingam, R. & Cohrs, R. J. (2000). Neurologic complications of the reactivation of varicella-zoster virus. *N Engl J Med* **342**, 635–645.

Gilden, D. H., Cohrs, R. J. & Mahalingam, R. (2003). Clinical and molecular pathogenesis of varicella virus infection. *Viral Immunol* **16**, 243–258.

Jenner, R. G., Alba, M. M., Boshoff, C. C. & Kellam, P. (2001). Kaposi's sarcoma-associated herpesvirus latent and lytic gene expression as revealed by DNA arrays. *J Virol* **75**, 891–902.

Kennedy, P. G. E. (2002). Varicella-zoster virus latency in human ganglia. *Rev Med Virol* **12**, 327–334.

Kennedy, P. G. E., Major, E. O., Williams, R. K. & Straus, S. E. (1994). Down-regulation of glial fibrillary acidic protein expression during acute lytic varicella-zoster virus infection of cultured human astrocytes. *Virology* **205**, 558–562.

Kennedy, P. G. E., Grinfeld, E. & Gow, J. W. (1998). Latent varicella-zoster virus is located predominantly in neurons in human trigeminal ganglia. *Proc Natl Acad Sci U S A* **95**, 4658–4662.

Kennedy, P. G. E., Grinfeld, E. & Bell, J. E. (2000). Varicella-zoster virus gene expression in latently infected and explanted human ganglia. *J Virol* **74**, 11893–11898.

MacLean, C. A., Clark, B. & McGeoch, D. J. (1989). Gene UL11 of herpes simplex virus type 1 encodes a virion protein which is myristylated. *J Gen Virol* **70**, 3147–3157.

Major, E. O., Miller, A. E., Mourrain, P., Traub, R. G., de Widt, E. & Sever, J. (1985). Establishment of a line of human fetal glial cells that supports JC virus multiplication. *Proc Natl Acad Sci U S A* **82**, 1257–1261.

McMillan, D. J., Kay, J. & Mills, J. S. (1997). Characterization of the proteinase specified by varicella-zoster virus gene 33. *J Gen Virol* **78**, 2153–2157.

Ng, T. I. & Grose, C. (1992). Serine protein kinase associated with varicella-zoster virus ORF 47. *Virology* **191**, 9–18.

Ng, T. I., Keenan, L., Kinchington, P. R. & Grose, C. (1994). Phosphorylation of varicella-zoster virus open reading frame (ORF) 62 regulatory product by viral ORF 47-associated protein kinase. *J Virol* **68**, 1350–1359.

Sommer, M. H., Zagha, E., Serrano, O. K. & 10 other authors (2001). Mutational analysis of the repeated open reading frames, ORFs 63 and 70 and ORFs 64 and 69, of varicella-zoster virus. *J Virol* **75**, 8224–8239.

Spengler, M., Niesen, N., Grose, C., Ruyechan, W. T. & Hay, J. (2001). Interactions among structural proteins of varicella zoster virus. *J Arch Virol Suppl* **17**, 71–79.

Stingley, S. W., Ramirez, J. J., Aguilar, S. A., Simmen, K., Sandri-Goldin, R. M., Ghazal, P. & Wagner, E. K. (2000). Global analysis of herpes simplex virus type 1 transcription using an oligonucleotide-based DNA microarray. *J Virol* **74**, 9916–9927.

Sun, A., Devi-Rao, G. V., Rice, M. K., Gary, L. W., Bloom, D. C., Sandri-Goldin, R. M., Ghazal, P. & Wagner, E. K. (2004). Immediate-early expression of the herpes simplex virus type 1 ICP27 transcript is not critical for efficient replication in vitro or in vivo. *J Virol* **78**, 10470–10478.

Wagner, E. K., Ramirez, J. J., Stingley, S. W., Aguilar, S. A., Buehler, L., Devi-Rao, G. B. & Ghazal, P. (2002). Practical approaches to long oligonucleotide-based DNA microarray: lessons from herpesviruses. *Prog Nucleic Acid Res Mol Biol* **71**, 445–491.

Yang, W. C., Devi-Rao, G. V., Ghazal, P., Wagner, E. K. & Triezenberg, S. J. (2002). General and specific alterations in programming of global viral gene expression during infection by VP16 activation-deficient mutants of herpes simplex virus type 1. *J Virol* **76**, 12758–12774.